Numerical and Experimental Results of Auxiliary Bearings Testing on a High Speed Test Rig

Tim Collins[a], Andrea Masala[a], Richard Shultz[a], Zenglin Guo[a]

[a] Waukesha Magnetic Bearings, Unit K, Lyons Way, Worthing - UK,
tcollins@waukbearing.com, amasala@waukbearing.com.com, rshultz@waukbearing.com, zguo@waukbearing.com

Abstract—A test stand including a rotor and active magnetic bearing system, located at Waukesha Magnetic Bearing premises was utilized in 2013 to validate a new auxiliary bearing design. This paper provides an overview of the preparatory activities and an insight on the numerical and experimental results obtained during the testing campaign.

I. INTRODUCTION

Auxiliary bearing systems are used on active magnetic bearing supported rotors to protect the rotor and stator part of the machine in case of overload of the active magnetic bearings (AMB) or failure of the AMB system resulting in a rotor drop or landing event. The auxiliary bearing system always includes a radial bearing system, two per rotor, and most often also an axial auxiliary bearing system. Different auxiliary bearing designs have been developed and tested over the years by Waukesha Magnetic Bearings (WMB) to meet specific customer and project requirements dictated by gas environment properties, rotordynamic performances and auxiliary bearing lives.

With reference to the radial auxiliary bearings, these can be classified in three main categories: bushing type, ball bearing type and hybrid type. The bushing type auxiliary bearing system (RDS) typically consists of a fixed stator part made of bearing pads mounted in a supporting housing by means of a compliant mounting system, and landing sleeve forming the rotor part.

A new type of auxiliary bearing landing sleeve was developed by Waukesha Magnetic Bearings in partnership with a major turbomachinery OEM using a new material and manufacturing process. The new auxiliary bearing design was intended to provide enhanced mechanical properties to enable the extension of this type of application to high speed rotors, and guarantee stability of performance over time.

The design and validation of the mechanical properties of the new auxiliary bearing sleeve was conducted in 2012 and was finalized in 2013 with an extensive test campaign on a test facility, prior to being approved for testing on the full scale machine.

The testing campaign, which included a repetition of a set of full speed rotor drops, was performed on a large size rotor test stand located at WMB premises and with capability to rotate a 1500 kg rotor up to 8000 rpm. The landing test and subsequent visual inspection and non destructive testing (NDT) confirmed successful results of the auxiliary bearing performance and good agreement between the predicted and measured results in terms of rotor drop dynamics and coefficient of friction at the rotor-stator interface.

Figure 1. RDS type radial auxiliary bearings

A summary of the test stand features, conditions and results are discussed here.

II. ENHANCED RADIAL AUXILIARY BEARINGS

RDS auxiliary bearings typically include separate radial and axial auxiliary bearing systems.

Radial RDS auxiliary bearings include a stator part consisting of a housing structure with compliantly mounted pads lined with a dry-self lubricating material, and a rotor part consisting of the landing sleeve which represents the journal part of the bearing system and provides the sliding contact interface with the lining of the stator part during a landing event or momentary contact. A schematic of the radial RDS auxiliary bearing is represented in Figure 2.

During normal operation of the AMB the rotor and stator parts of the auxiliary bearings are not in contact and a nominal gap, normally ranging between 0.2 and 0.35 mm will be present.

During a landing event, the rotor will move away from its nominal centered position, resulting with a contact with the stator parts. The RDS type auxiliary bearing provides a frictional sliding bearing surface to allow the rotor to coast down safely to rest. This process results in high thermal energy input to the auxiliary bearing landing sleeve and wear to the stator pad material. The endurance of the landing sleeve and stator pads depends on the capacity of the material to dissipate the thermal energy generated during the landing event.

The original auxiliary bearing sleeve design was based on a bronze/copper alloy characterized by high thermal conductivity and diffusivity properties which resulted in a relatively low temperature rise of the auxiliary bearing system during a landing event.

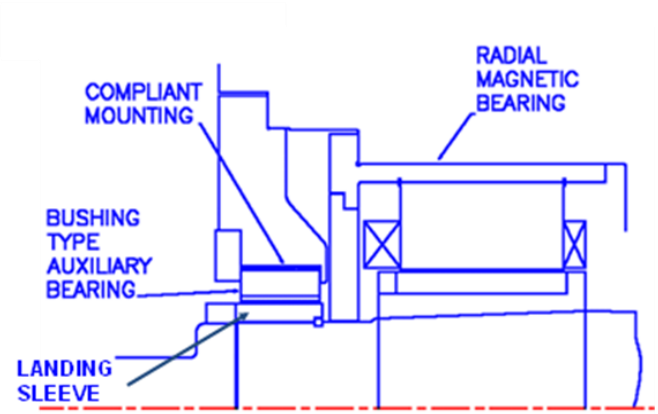

Figure 2. RDS type radial auxiliary bearings

The requirement to keep the landing sleeves in contact with the shaft when the machine is rotating at maximum speed with the worst case temperature gradient coupled with consideration of manufacturing tolerances sets the requirement for a robust interference fit between the landing sleeve and shaft. The resulting hoop stresses generated during the assembly process or during rotational operation may limit the application of RDS type auxiliary bearing systems for high speed machines.

To overcome this limitation, a new landing sleeve design was developed in cooperation with a major turbomachinery OEM. The new sleeve design (Figure 3) consists of a bi-metallic sleeve and is composed of an outer landing sleeve, which utilises a material with high thermal conductivity and diffusivity properties, bonded to an inner carrier sleeve, which utilises a material with higher strength characteristics, where higher stress levels are present.

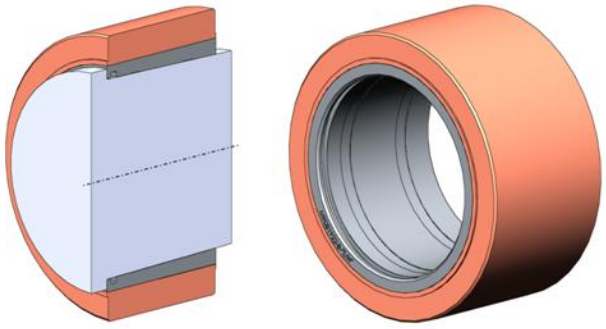

Figure 3. The new sleeve design

The design of the landing sleeve was verified with detailed Finite Element Analysis, able to predict the temperature profile of the sleeve and rotor by means of transient and non-linear analysis during a landing event from full speed.

III. TEST RIG DESCRIPTION

To validate the new landing sleeve design an experimental activity, including repetition of landing tests representative of a real high speed / heavy weight rotor were performed. The landing tests were performed on an existing stand, located on a confined and protected area at WMB premises. The test stand, known as the 'Red Rig' because of the characteristic color of the shielding structure is pictured in Figure 4. The Red Rig was originally developed in the late '90s by the company with the purpose of verifying AMB and auxiliary bearing performance when subject to shock loads.

Figure 4. The Red-Rig test stand

A schematic of the Red-Rig is represented in Figure 5. The red rig has a horizontal rotor supported by two radial AMBs and two split axial AMBs (with a thrust disc on each end of the rotor). Besides each radial AMB are located the two RDS type radial auxiliary bearings. The axial auxiliary bearing is located at the NDE of the rotor. The Red Rig includes an external shaker system to excite the rotor, when at standstill, at different position, and several emergency braking systems to absorb rotational energy from the rotor in case of a failure of the AMB or auxiliary bearing systems during the test.

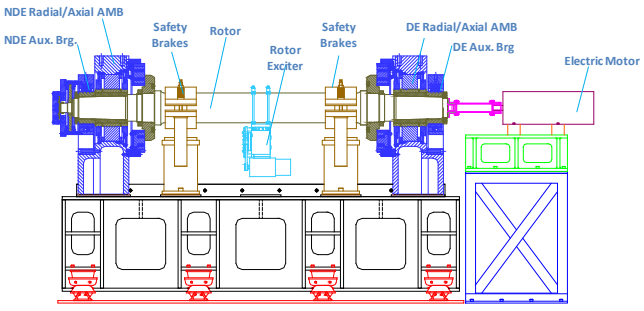

Figure 5. Red Rig rotor and AMB system schematic

Featuring a 1500 kg supercritical rotor, running up to 8000rpm, and able to accommodate some of the latest electronic and software capabilities developed by WMB over the years, such as auto-clearance check, remote commissioning and more recently auto-tuning capabilities, the Red-Rig was used over the years as a permanent laboratory able to reproduce some of the critical aspects

that a rotor or AMB system will experience during real operation.

To perform the landing test repetitions required to validate the new landing sleeves design, while being able to guarantee the required level of safety for the equipment and personnel involved in the test, red rig was re-commissioned and operated under strict safety rules and verification procedures. These were based on a well developed pre-existing risk assessment and safety justification.

The commissioning included rotor balancing and AMB tuning operations to keep residual or desired unbalance levels and vibrations under strict control. Fine measurements of residual clearances and monitoring of landing sleeves temperature during operation and following a landing event were made.

IV. NUMERICAL SIMULATIONS

Prior to performing the testing activity on the new landing sleeve design, an extensive numerical activity was performed to predict the rotor drop results and determine the test conditions to have similitude between the test rig and the actual machine.

The simulations accounted for different phenomena related to the rotor auxiliary bearing performances during a landing event, including rotor drop dynamics and loads, transient thermal effects and stress analysis on the rotor sleeves.

The transient rotor drop dynamic simulation was performed by means of WMB proprietary numerical tools, which combine the rotor dynamics with the auxiliary bearing characteristics, including compliance system stiffness effects and, friction and contact models between rotor and auxiliary bearings.

A finite element model of the red rig rotor is represented in Figure 6. The model includes AMBs and auxiliary bearing systems and allows the determination of the rotor vibration amplitudes on selected rotor stations, and loads on the AMBs and auxiliary bearings to be transferred to the thermal and stress analysis.

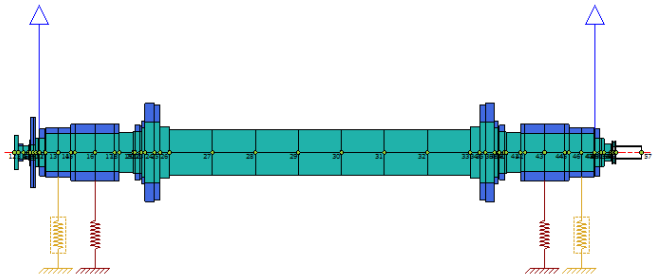

Figure 6. FEM model of the Red-Rig rotor

Different unbalance configurations, with a total unbalance equivalent to ISO G 2.5 were considered on the simulation runs. The transient responses of the system during a landing event with unbalances located on the two opposite shaft ends and in phase are shown in Figure 7 and Figure 8 where the bearing clearance and compliance circles are marked in green and red respectively.

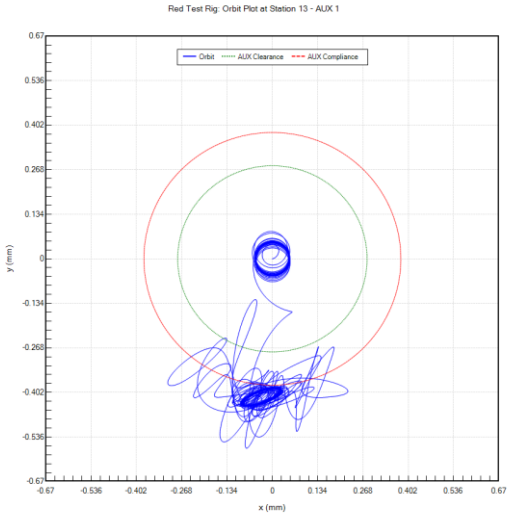

Figure 7. Rotor orbit at NDE

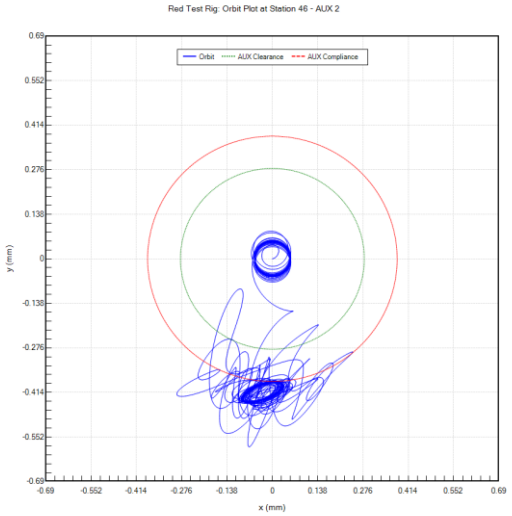

Figure 8. Rotor orbit at DE

Detailed thermal and structural FE analyses were necessary to investigate the performance of the new sleeve design during the normal operating cycles of the machine and during the worst case landing event from the maximum operating speed.

The analysis of normal operating cycles considered variations in operating speed and temperature conditions along with the interference boundary condition and utilized a non-linear material model to establish plastic strain cycles at the bonding interface between landing and carrier sleeves.

The landing event analysis utilised a combined thermal transient and structural FE model. The temperature distribution in the sleeves resulting from thermal energy input due to the frictional sliding interface between rotor and stator parts of the auxiliary bearing system were simulated during the landing transient to ensure that peak operating temperatures remained within allowable limits. Figure 9 shows a typical temperature distribution during a landing event,

Temperature distributions from the thermal transient analysis were mapped onto a structural FE mesh to study the resultant stress state within the sleeves along with

interference fit and centrifugal loading during the landing event. Resulting contact pressures at the interference fits and thermal expansions at the sleeve ODs provided key justifications for determining the safe conditions to run the test.

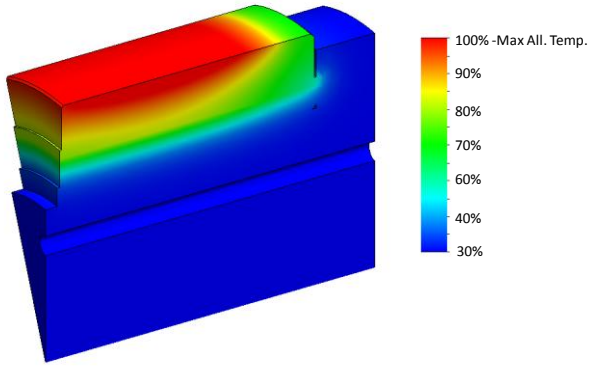

Figure 9. Typical temperature distribution during a landing event.

V. THE TEST PROGRAM

The commissioning and test programs were completed in a step wise manner where landing tests were completed from increasingly higher speeds. The braking systems and dynamic behavior of the RDS auxiliary bearing system were validated at each stage against the predicted behavior.

Test speeds were determined using an energy equivalency principle where the thermal energy input due to friction per unit volume of the landing sleeves was compared to that of the full sized machine.

To further guarantee the equivalency between the test and a landing event on the full sized machine it was necessary to apply an external braking torque to the rotor during the landing tests, This braking torque was provided by a combination of regenerative braking from the electric motor drive and a frictional braking torque developed by the axial auxiliary bearing. To this aim the axial AMB actuator was maintained active and able to develop a known amount of force and braking torque, during the landing test. In total, two levels of braking torque were used during the test program in order to study the coefficient of friction at the rotor-stator interface.

Using the energy equivalency principle it was determined that a landing test from 6000 rpm on the red rig with medium braking torque is equivalent to a landing event from maximum operating speed on the full sized machine.

Non contacting infrared temperature sensors were targeted at the OD surface of each auxiliary bearing sleeve. Sensor outputs were logged to give an indication of temperature rise during rotational operation and landing tests.

The diagnostic outputs from the AMB controller were logged to capture the rundown speed curves and rotor positions during the landing tests. This data was used to calculate the coefficient of friction in the radial auxiliary bearings and review radial stator pad wear behavior.

VI. TEST RESULTS

The landing test speeds, durations and energy inputs per unit volume of landing sleeve material used during the test program are given in Figure 10.

Speed (rpm)	Breaking Torque Level	Duration (s)	Energy Input (J mm^-3)
3200	Medium	27	0.172
5000	Medium	32	0.295
6000	Medium	34	0.369
6000	High	19	0.208
7500	High	17	0.275
7500	High	15	0.185
7600	High	17	0.237

Figure 10. Landing test speeds, durations and energy inputs.

Knowledge of the torque generated by the braking systems along with the speed-time curves for each landing test was used to calculcate the coefficient of friction at the rotor-stator interface. Figure 11 shows typical plot of coefficient of friction against speed for a landing test from 5000 rpm. The plot shows that coefficient of friction was in the range of 0.055 to 0.080 for the region where the rotor runs down from 4600 to 2000 rpm. This result is in good agreement with previous landing tests and data from the field.

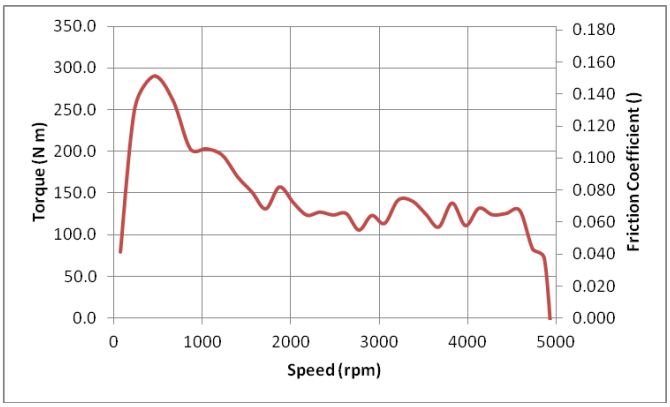

Figure 11. Friction Coefficient for 5000 rpm Landing Test

The rotor orbits were measured with fast dynamic signal and recorded for each landing event. The rotor drop orbits corresponding to the drop conditions measured during the landing event at 7600 rpm is represented in Figure 12. The rotor orbit showed a typical pendulum motion after some initial bouncing. Importantly no insurgence of backward or forward whirl was identified. The measured results were generally in good agreement in terms of vibration amplitudes with the simulation results represented in Figure 13.

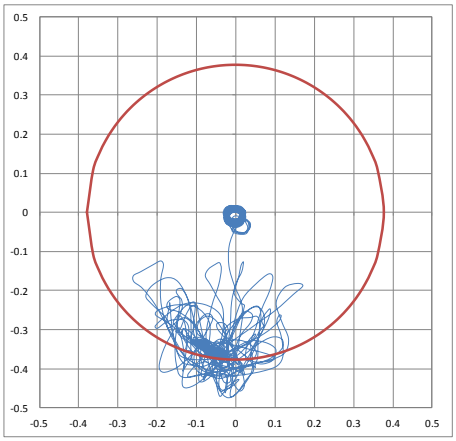

Figure 12. Measured orbit at the NDE Sensor

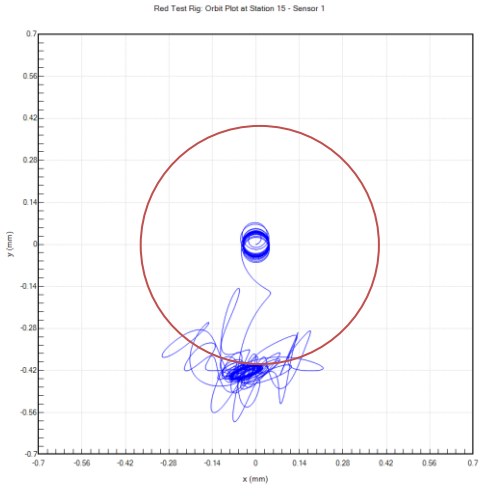

Figure 13. Simulated orbit at the NDE Sensor

VII. VISUAL INSPECTION AND NDT RESULTS

The auxiliary bearing stator pads were measured before and after each landing test to establish the degree of wear that occurred. Figure 14 shows the cumulative wear for lower pads of the auxiliary bearing stators after three successive landing tests from high speed.

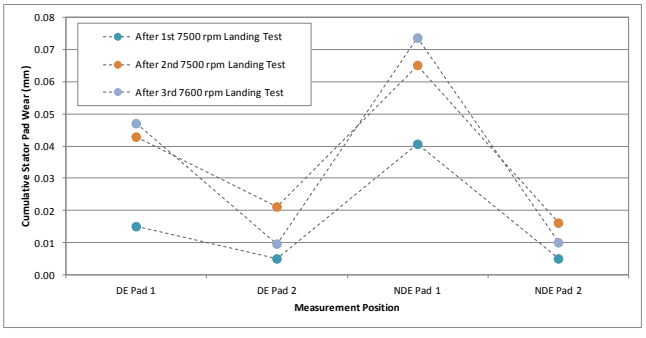

Figure 14. Cumulative pad wear

The figure shows that the wear rates were relatively low with the majority of wear being limited to within 0.08 mm across the high speed landings. The phenomenon whereby the stator bore reduces after landing tests/events has been witnessed previously during testing and in the field. This is a result of material transfer from other positions around the stator and from deposits on the rotor from previous landing tests. In general, the wear rates and behavior experienced during the landing tests on the red rig were consistent with experience of previous landing tests and landing events in the field.

The stator pad build up on the radial auxiliary bearing sleeve OD surfaces was measured at critical points during the test program. In general, the number of deposit patches increased with each landing test. Patches which existed before a landing test tended to increase in size and thickness during subsequent landing tests. After several high speed landing tests the majority of patched were found to be in the thickness range of 0.025 to 0.050 mm with the thickest being 0.080 mm.

Figure 15. Stator pad deposits on landing sleeve after 7600 rpm landing test.

Following the completion of the test program the radial auxiliary bearing sleeves were subjected to a detailed inspection to ensure that no defects had developed during the testing which would compromise their structural integrity for continued operational use. A 100% dye penetrant inspection was performed to examine for surface breaking flaws on the sleeve OD. An image of the NDE landing sleeve is represented in Figure 16. A 100% ultrasonic inspection was performed to check the integrity of the bonding between the carrier and landing sleeves portions of the sleeve. No referable indications of damage or flaws were observed during either of the inspections.

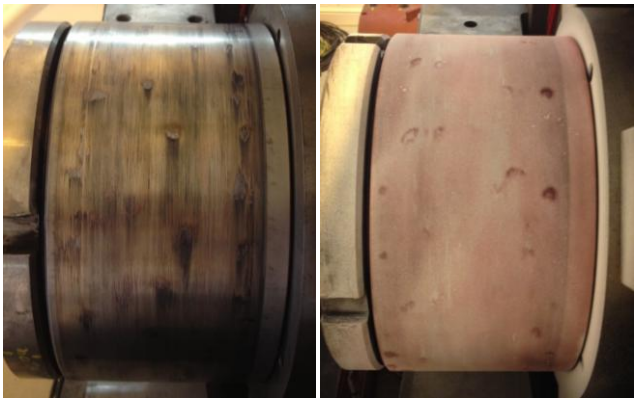

Figure 16. NDE Sleeve after Dye Penetrant Inspection

VIII. SUMMARY

Analysis of the diagnostic outputs from the AMB controller during the landing events show that the dynamic behavior of the auxiliary bearing system was as predicted and consistent with experience of previous landing tests and landing events in the field

In summary, the testing of the scale model sleeves on the red rig was successful and the sleeves proved fit for purpose. The new auxiliary bearing sleeve design was qualified for testing on the full sized machine on the basis of this successful testing.

REFERENCES

[1] S. Yates, R.R. Shultz, Landing, "Test Results for a 6 MW Motor Compressor and Auxiliary Bearing Systems for Corrosive Environments", *Proceedings of 13th International Symposium on Magnetic Bearings*, 2012.

[2] R.R. Shultz, E. Lucchetta, "Time transient simulation model and full scale experimental verification for high speed rotor delevitation events with a 1.5 ton supercritical rotor supported by dry lubricated bushing type auxiliary bearings" - *Proceedings of International Conference on Compressors and Their Systems*, 2005.